

## **ACTIVATED CARBON COMPOSITES FOR AIR SEPARATION**

Frederick S. Baker

Oak Ridge National Laboratory, Bethel Valley Road, P. O. Box 2008, Oak Ridge, TN 37831-6087

E-mail: [bakerfs@ornl.gov](mailto:bakerfs@ornl.gov); Telephone: (865) 241-1127; Fax: (865) 576-8424

Cristian I. Contescu

Oak Ridge National Laboratory, Bethel Valley Road, P. O. Box 2008, Oak Ridge, TN 37831-6087

E-mail: [contescuci@ornl.gov](mailto:contescuci@ornl.gov); Telephone: (865) 241-3318; Fax: (865) 576-8424

Costas Tsouris

Oak Ridge National Laboratory, Bethel Valley Road, P. O. Box 2008, Oak Ridge, TN 37831-6087

E-mail: [tsourisc@ornl.gov](mailto:tsourisc@ornl.gov); Telephone: (865) 241-3246; Fax: (865) 241-4289

Joanna McFarlane

Oak Ridge National Laboratory, Bethel Valley Road, P. O. Box 2008, Oak Ridge, TN 37831-6087

E-mail: [burchelltd@ornl.gov](mailto:burchelltd@ornl.gov); Telephone: (865) 576-8595; Fax: (865) 576-8424

### **ABSTRACT**

Large-scale application of oxygen-blown coal gasification, currently the most effective and efficient approach for production of hydrogen from coal is still in need of a cost-effective means of enriching O<sub>2</sub> concentration in air. This project is focused on the development of activated carbon composites for the production of an oxygen-enriched air stream suitable for coal gasification. The method proposed exploits the molecular sieving properties of porous materials, including activated carbon. The potential to separate O<sub>2</sub> and N<sub>2</sub> from air is based on the different diffusion rates of the two molecules in the composite, which has been previously demonstrated. In addition, it has been recently discovered that the peculiar magnetic properties of O<sub>2</sub> molecules induce sizable magnetodesorption effects at equilibrium in a static system at room temperature and under moderate magnetic field intensity. The effects were attributed to a transition in the magnetic state of O<sub>2</sub> molecules; i.e., from paramagnetic in the gas phase to a non-magnetic state when confined in the micropores of the adsorbent. This effect was observed only when the carbon adsorbent was pre-loaded with super-paramagnetic nanoparticles of Fe<sub>3</sub>O<sub>4</sub>, and was explained attributed to the local enhancement of magnetic field caused by magnetite particles supported on the microporous adsorbent.

In continuation of the development of composite materials for air separation based on molecular sieving properties and magnetic fields effects, several molecular sieve materials were tested in a flow system, and the effects of temperature, flow conditions, and magnetic fields were investigated. New carbon materials adsorbents, with and without pre-loaded super-paramagnetic nanoparticles of Fe<sub>3</sub>O<sub>4</sub> were synthesized; all materials were packed in chromatographic type columns which were placed between the poles of a high intensity, water-cooled, magnet (4 Tesla). In order to verify the existence of magnetodesorption effect, separation tests were conducted by injecting controlled volumes of air in a flow of inert gas, while the magnetic field was switched on and off. Gas composition downstream the column was analyzed by gas chromatography and by mass spectrometry. Under the conditions employed, the tests confirmed that N<sub>2</sub> – O<sub>2</sub> separation occurred at various degrees, depending on material's intrinsic properties, temperature and flow rate. The effect of magnetic fields, reported previously for static conditions, was not confirmed in the flow system. The best separation was obtained for zeolite 13X at sub-ambient temperatures. Future directions for the project include evaluation of a combined system, comprising carbon and zeolite molecular sieves, and testing the effect of stronger magnetic fields produced by cryogenic magnets.

## INTRODUCTION

Carbon fiber composite molecular sieves (CFCMS) have been developed at Oak Ridge National Laboratory (ORNL) as a novel class of adsorbent which combines tailored gas adsorption properties, good gas permeability, and electrical conductivity.<sup>[1-3]</sup> The structure of CFCMS comprises carbon fibers (about 10  $\mu\text{m}$  in diameter) bonded at their contact points by a continuous carbon skeleton that is electrically conductive. The combination of open structure, microporosity, and electrical conductivity allows the material to be used in a regenerative, electrical swing adsorption (ESA) system.<sup>[4-6]</sup> This is the analog of pressure swing adsorption (PSA) where regeneration of the adsorbent is facilitated by resistive heating of the carbon monolith.

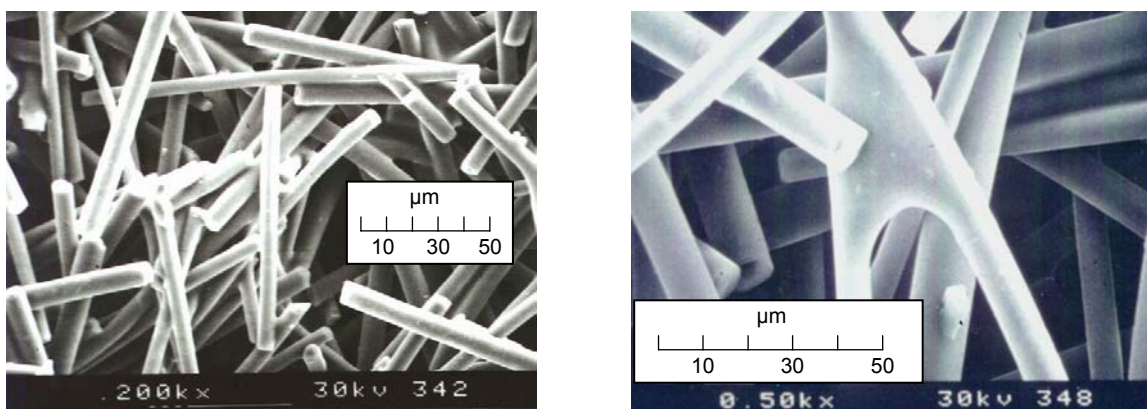


Figure 1 - SEM images showing the structure of CFCMS material

Preliminary work demonstrated that CFCMS material has the potential for separating  $\text{O}_2$  and  $\text{N}_2$  in air.<sup>[7]</sup> Further findings also indicated that the efficiency of separation could be increased by better tailoring the pore size distribution to very narrow micropore sizes ( $< 2$  nm). Based on characterization of a series of CFCMS samples, it was found that  $\text{O}_2$  was more rapidly adsorbed on the carbon fiber than  $\text{N}_2$ , and with higher equilibrium uptakes, provided the fiber contained a high proportion of very narrow micropores. The conclusion was that CFCMS activated under certain conditions is able to separate  $\text{O}_2$  and  $\text{N}_2$  from air based on kinetic effects, i.e. the difference in diffusion rates of the two molecules in the network of narrow micropores in the carbon fiber structure. Since  $\text{O}_2$  molecules are only slightly smaller in size than  $\text{N}_2$  molecules (their kinetic diameters are 3.62 nm and 3.80 nm), achieving selectivity requires a carbon molecular sieve with very narrow and well controlled pore size distribution in the critical range of 3-5 nm. Although controlling the pore size of carbon materials is achievable, the almost perfect separation selectivity offered by zeolites under favorable conditions is hard to match.

Addition of a magnetic field was also investigated in an attempt to further enhance the potential of molecular sieving effects. On theoretical grounds it was hypothesized that adsorption of  $\text{O}_2$  should be influenced by magnetic fields whenever adsorption is accompanied by a transition between paramagnetic and diamagnetic states. Although the literature on magnetic field effects on adsorption and desorption is scarce, several examples show that the occurrence of magneto-adsorption-desorption effects strongly depends on the nature of solids and gases, temperature, and the intensity of magnetic fields.<sup>[8-12]</sup> An appropriate combination of these factors could lead to a separation process based on selective adsorption from a mixture of gases. In this context it has been reported that separation of  $\text{O}_2$  and  $\text{N}_2$  in high magnetic fields is in principle plausible in a steady magnetic field through adsorption of paramagnetic  $\text{O}_2$  molecules into micropores of porous ferromagnetic solids.<sup>[13]</sup>

In order to verify this theoretical prediction, a series of measurements of O<sub>2</sub> adsorption isotherms was carried out in static, equilibrium conditions.<sup>[14]</sup> In preliminary tests it was found that the amount of O<sub>2</sub> adsorbed at equilibrium was lower (by about 6% at 0.1 MPa) in presence of a weak magnetic field (0.8 Tesla) than in absence of the magnetic field. Although small, this magnetodesorption effect was sizable and observed repeatedly at room temperature for activated carbon fibers loaded with 10 wt % of superparamagnetic magnetite nanoparticles (Fe<sub>3</sub>O<sub>4</sub>, average size 16 nm). The results of these preliminary tests motivated continuation of the project for additional verification and confirmation of the effect at higher magnetic field intensities and in dynamic conditions; in the new series of tests reported here, a flow system, rather than static, was used to better simulate the conditions of air separation for practical applications. Tests for air separation in absence of a magnetic field were also carried out.

## DISCUSSION OF CURRENT ACTIVITIES

### MATERIAL PREPARATION AND CHARACTERIZATION

#### Carbon Fiber Composite Molecular Sieves (CFCMS)

A series of CFCMS composites were used as support for loading a dispersed magnetic phase, magnetite. The CFCMS materials were selected based on their microporous structure and BET surface area values.<sup>[15]</sup> The surface and porosity properties were characterized by adsorption of N<sub>2</sub> at 77 K and by adsorption of CO<sub>2</sub> at 273 K.<sup>[16]</sup> All adsorption measurements were made using the Autosorb 1 instrument (Quantachrome). Adsorption data were further processed to calculate the pore size distribution of porosity and surface areas using the density functional theory (DFT) in the non-local density approximation.<sup>[16-19]</sup> The DFT software available from Quantachrome was used for calculations. Figures 1 and 2 show the results of pore size distribution in form of cumulative and differential plots. The results obtained from N<sub>2</sub> adsorption at 77 K (lowest accessible pores ~ 10 Å) and CO<sub>2</sub> adsorption at 273 K (pores between 3 and 12 Å) are overlapped in both plots.

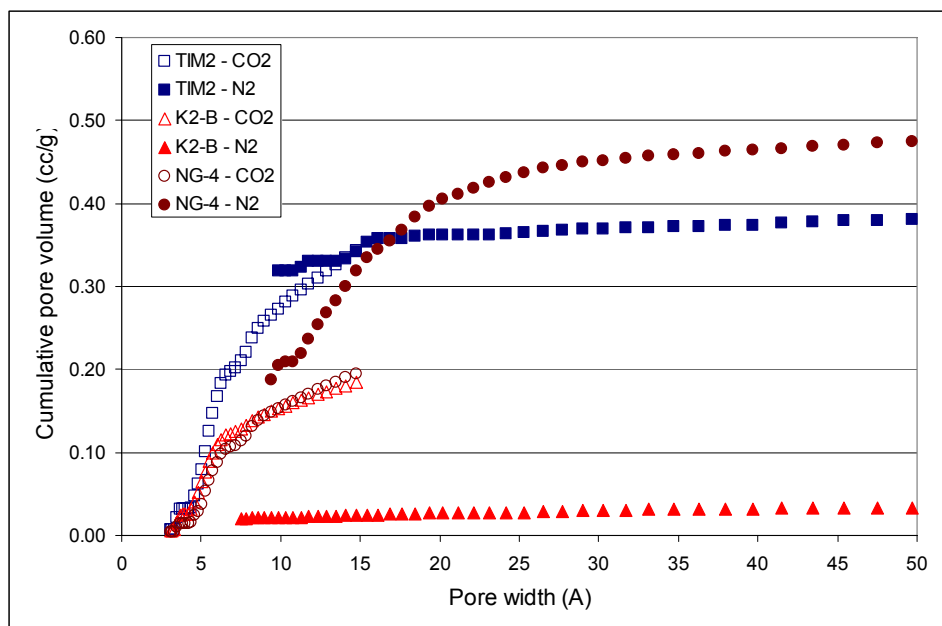


Figure 1: Cumulative pore volume distribution as a function of pore widths. Data calculated by DFT method from N<sub>2</sub> adsorption and CO<sub>2</sub> adsorption are plotted on a common scale.

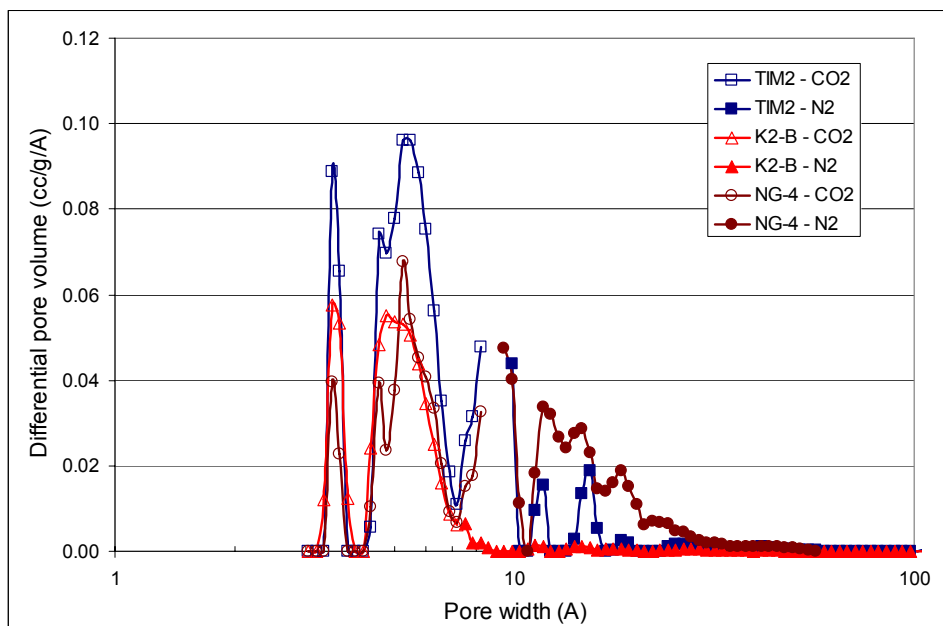


Figure 2: Differential distribution of pore volume as a function of pore width. Data calculated by DFT method from N<sub>2</sub> adsorption and CO<sub>2</sub> adsorption are plotted on a common logarithmic scale.

The results presented in Table 1 include the surface area values calculated from N<sub>2</sub> adsorption data using the BET equation, and from the N<sub>2</sub> and CO<sub>2</sub> adsorption data using the DFT method; the pore volume calculated from N<sub>2</sub> and CO<sub>2</sub> adsorption data using the DFT method; and the average pore width calculated from the same adsorption data using the DFT method. Comparing the results reveals several differences between the three samples:

- Sample NG-4 has a relatively large surface area based on BET result (1123 m<sup>2</sup>/g) and DFT result from N<sub>2</sub> adsorption (923 m<sup>2</sup>/g). In contrast, CO<sub>2</sub> adsorption reveals lower surface area (600 m<sup>2</sup>/g), suggesting blockage of pore entrance by bulky oxidized surface groups, that may have been formed during the activation process.
- Sample TIM-2 has a slightly lower BET surface area (964 m<sup>2</sup>/g) and the DFT results for N<sub>2</sub> adsorption (960 m<sup>2</sup>/g) and CO<sub>2</sub> adsorption (1090 m<sup>2</sup>/g) are not much different. For this sample, both molecular probes used as adsorbate (N<sub>2</sub> and CO<sub>2</sub>) give essentially the same pore volume (0.34 – 0.39 cc/g), which is a strong indication that the material is largely microporous. Indeed, the average pore width calculated by DFT method is 9.8 Å (based on N<sub>2</sub> adsorption) or 5.2 Å (based on CO<sub>2</sub> adsorption).
- Sample K2-B has a very small surface area value based on N<sub>2</sub> adsorption data (73 m<sup>2</sup>/g from BET equation; 85 m<sup>2</sup>/g from DFT method). This contrasts with the large surface area measured by CO<sub>2</sub> adsorption (640 m<sup>2</sup>/g based on DFT method), and is a strong evidence that the material contains very narrow micropores that cannot be accessed by N<sub>2</sub> at 77 K, but are accessible to CO<sub>2</sub> at 273 K. With an average pore width of 7.5 Å (based on N<sub>2</sub> adsorption) or 3.5 Å (based on CO<sub>2</sub> adsorption), the K2-B material is expected to have the most pronounced molecular sieving properties.

Distribution of porosity by pore width is different for the three materials. While all carbons have narrow micropores between 5 and 7 Å (Fig. 2), the corresponding volume is larger for sample TIM-2 than for

samples K2-B and NG-4. In addition, samples TIM-2 and NG-4 have large micropores in the range of 7 – 20 Å; this range of micropores is missing from sample K2-B.

**Table 1** Surface area and porosity characteristics of base CFCMS materials selected for tests

CFCMS	Surface area			Pore volume		Average pore width	
	BET N2 m <sup>2</sup> /g	DFT N2 m <sup>2</sup> /g	DFT CO2 m <sup>2</sup> /g	DFT N2 cc/g	DFT CO2 cc/g	DFT N2 A	DFT CO2 A
NG 4	1123	923	600	0.476	0.195	9.4	5.2
TIM 2	964	960	1090	0.394	0.344	9.8	5.2
K2-B	73	85	640	0.035	0.185	7.5	3.5

### Magnetite-loaded CFCMS

As explained in the Introduction, previous results have shown that moderate intensity magnetic fields affect the adsorption of O<sub>2</sub> at equilibrium (at room temperature and maximum 0.1 MPa) on magnetite-loaded microporous activated carbon composites (CFCMS).<sup>[14]</sup> The effect was explained<sup>[20]</sup> on thermodynamic grounds after Ozeki and Sato<sup>[13]</sup> assuming that the magnetic state of O<sub>2</sub> confined in narrow micropores of activated carbon changes from paramagnetic (for free O<sub>2</sub>) into random magnetism (for O<sub>2</sub> clusters confined). The decrease of magnetization manifested in presence of an applied magnetic field is expected to induce an increase in pressure (i.e., desorption) of O<sub>2</sub>. The effect is too weak to be observed on pure microporous adsorbents (such as CFCMS), but was observed in static conditions with magnetite-doped CFCMS, because of the local enhancement of magnetic fields in nanopores induced by superparamagnetic Fe<sub>3</sub>O<sub>4</sub> nanoparticles.<sup>[14]</sup>

In order to verify the occurrence of this effect in dynamic conditions, a series materials loaded with Fe<sub>3</sub>O<sub>4</sub> were synthesized. The carbon supports selected were two granular mesoporous carbons derived from wood (WV A-1500 and SA-30, both from MeadWestvaco) and the CFCMS sample NG-4. The cold precipitation method used previously<sup>[21]</sup> was employed for loading magnetite on these carbons. The method consists essentially in precipitation of Fe<sub>3</sub>O<sub>4</sub> from aqueous solutions containing Fe(NO<sub>3</sub>)<sub>3</sub> and FeSO<sub>4</sub> in the stoichiometric ratio Fe<sup>III</sup> : Fe<sup>II</sup> = 2:1 necessary for formation of the mixed oxide Fe<sup>III</sup><sub>2</sub>O<sub>3</sub>.Fe<sup>II</sup>O. The precipitation agent is concentrated ammonia solution and the precipitation occurs at pH 10-11. No heating is necessary. In contrast with the ceramic method for synthesis of magnetite, which involves high temperature processes and results in a highly sintered product, the cold synthesis method preserves the nanosized colloidal particles of magnetite.

It was found that the above procedure can be used with the CFCMS sample NG-4, yielding uniformly loaded carbon particles (about 1 – 1.5 mm in size) and a clear residual solution that contained only traces of iron salts. The Fe-NG-4 sample (10 % Fe<sub>3</sub>O<sub>4</sub>) was obtained by this method. X-ray analysis showed the presence of a Fe<sub>3</sub>O<sub>4</sub> phase with small average crystallite size. However, the precipitation method described above could not be used with the wood-derived mesoporous carbons because of their high phosphorus content. It was found that these carbons have been activated with phosphoric acid, and the residual phosphorus on their surface perturbed the precipitation reactions leading to formation of Fe<sub>3</sub>O<sub>4</sub> in presence of ammonia as described above. Rather than leading to homogeneous deposits of magnetite on carbon, preferential complexation of Fe<sup>III</sup> by surface phosphorus caused deposition of Fe<sub>2</sub>O<sub>3</sub> (non magnetic) and precipitation of ferrous hydroxide in the aqueous phase.

## **Zeolite**

A granular sample of zeolite X13 was also used for air separation tests in the flow system. Before packing in a chromatographic-type column, zeolite beads (1.5 - 2 mm) were pretreated at 140 °C for dehydration.

## **Experimental setup**

All adsorbents in form of granules (1-2 mm) were packed in chromatography-type columns (copper tube, 50 cm long, ¼ inch diameter) which were rolled into a 3-coils spiral (5 cm diameter) that was placed flat between the poles of a water-cooled electromagnet (Applied Magnetics Lan, model 2V1). The maximum field intensity between the magnet poles was 1.5 Tesla.

Before packing in chromatography-type columns, all adsorbents were pre-dried overnight at 140 °C. After packing in the column all adsorbents were conditioned overnight in a flow of He (50 cc/min) at 150 – 200 °C. After conditioning the adsorbent, the flow of He was adjusted to the desired value for air separation tests (15 – 30 cc/min). The tests were performed by injecting controlled volumes of air through a septum upstream of the adsorbent column, and analyzing the composition of the gas exiting from the column.

In a first series of tests the gas composition analysis was performed with a Hewlett Packard 5890 series II gas chromatograph (GC) equipped with thermal conductivity (TC) detector. The chromatograph was operated by Agilent ChemStation software for GC systems. It was found that the difference between thermal conductivities of oxygen and nitrogen is not large enough to afford separate identification of the components in a mixture using the TC detector. To correct that, the GC analysis of gas composition downstream the adsorbent column was replaced later by analysis by mass spectroscopy. A Vacuum Technology Inc. mass spectrometer (MS) was used, which was operated by the manufacturer's software (VTI). The instrument was connected through a flow controlling valve and capillary tube to a derivation of the main gas line downstream the adsorbent column. This latter setup was proven more efficient for separate detection of oxygen and nitrogen concentration breaking through the column after air injection, even though the two components were poorly separated on the column.

## **AIR SEPARATION BASED ON MOLECULAR SIEVING EFFECTS**

### **Carbon fiber composite molecular sieves (CFCMS)**

Figure 3 shows examples of mass spectrometer signals for N<sub>2</sub> (blue line) and O<sub>2</sub> (red line) recorded after the breakthrough of air following an injection of 5 cc in a flow of He (30 cc/min) through a 50 cm long column filled with CFCMS TIM-2. The tests were done at various temperatures and at constant flow rate, which was vented out at atmospheric pressure. The pressure shown on this plot (in the range of 10<sup>-5</sup> Torr) is the actual pressure in the mass spectrometer chamber.

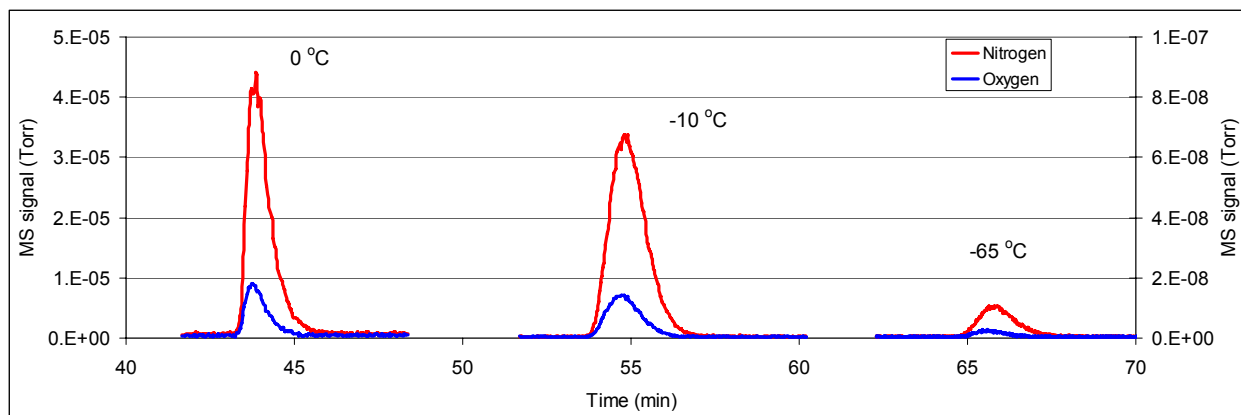


Figure 3: Example of breakthrough nitrogen and oxygen mass spectrometer signals measured for sample TIM-2 after injection of 5 mL air at various temperatures. Flow rate of He carrier was 30 cc/min.

The result of Fig. 3 shows that the peaks corresponding to  $N_2$  and  $O_2$  exiting the column were overlapped. The area under each peak corresponds to the concentration of that component in the mixture and reflects the air composition (roughly 21 vol %  $O_2$ ; 79 vol %  $N_2$ , traces of Ar,  $CO_2$   $H_2O$  etc). In order to better evaluate the effectiveness of  $N_2 - O_2$  separation, the mass signals for  $N_2$  and  $O_2$  were normalized to the peak maximum of each component; the results for four different temperatures are shown in Fig. 4.

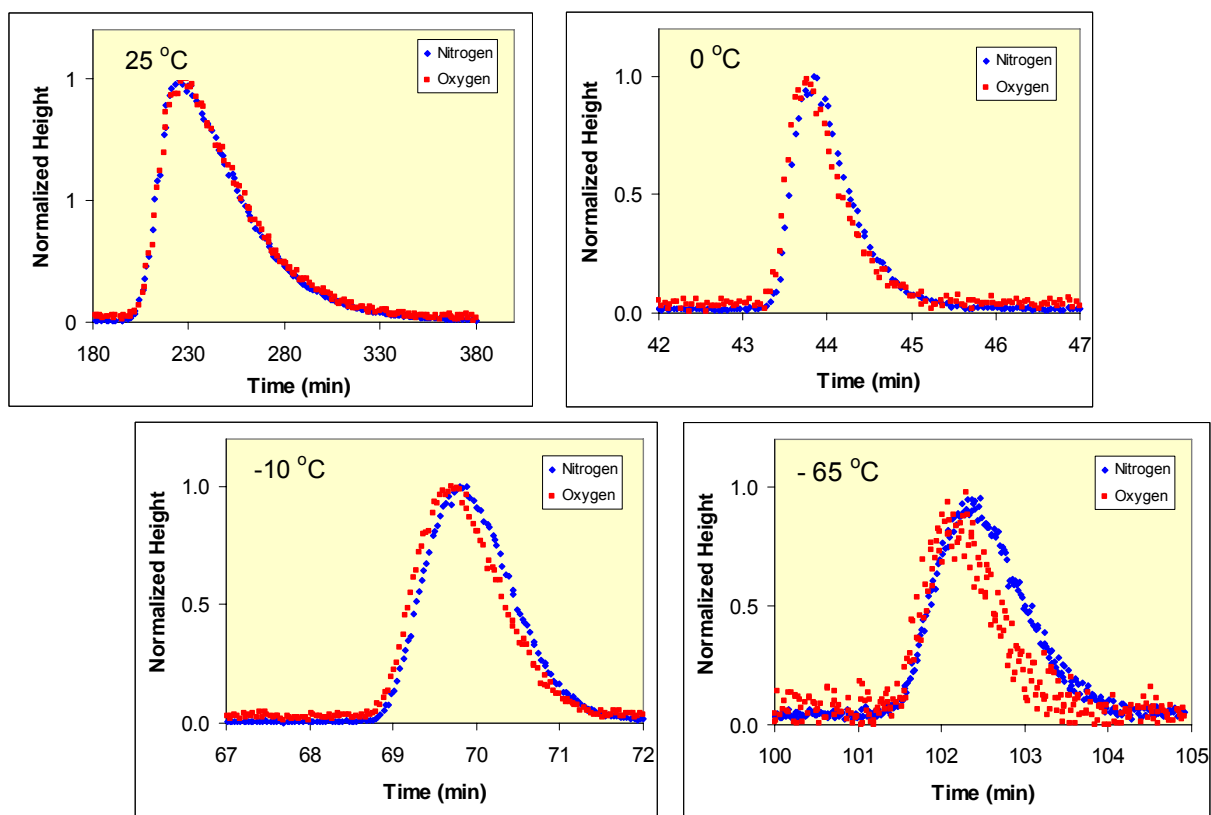


Figure 4: Normalized mass spectrometer signals for  $N_2$  (blue) and  $O_2$  (red) breaking through a 50 cm column packed with CFCMS TIM-2 material after injection of air at various temperatures. The flow rate of carrier gas (He) was 30 cc/min.

This test result shows that (1) separation of  $N_2 - O_2$  is possible, with the  $N_2$  peak being delayed with respect to the  $O_2$  peak; (2) the delay of  $N_2$  peak increases as the temperature is lowered below room temperature; (3) the efficiency of separation was not high enough in the test conditions selected, but could be improved by adjusting the flow rate, length of column, and the size of injection.

Figure 5 shows the results of a similar test with the CFCMS material K2-B.

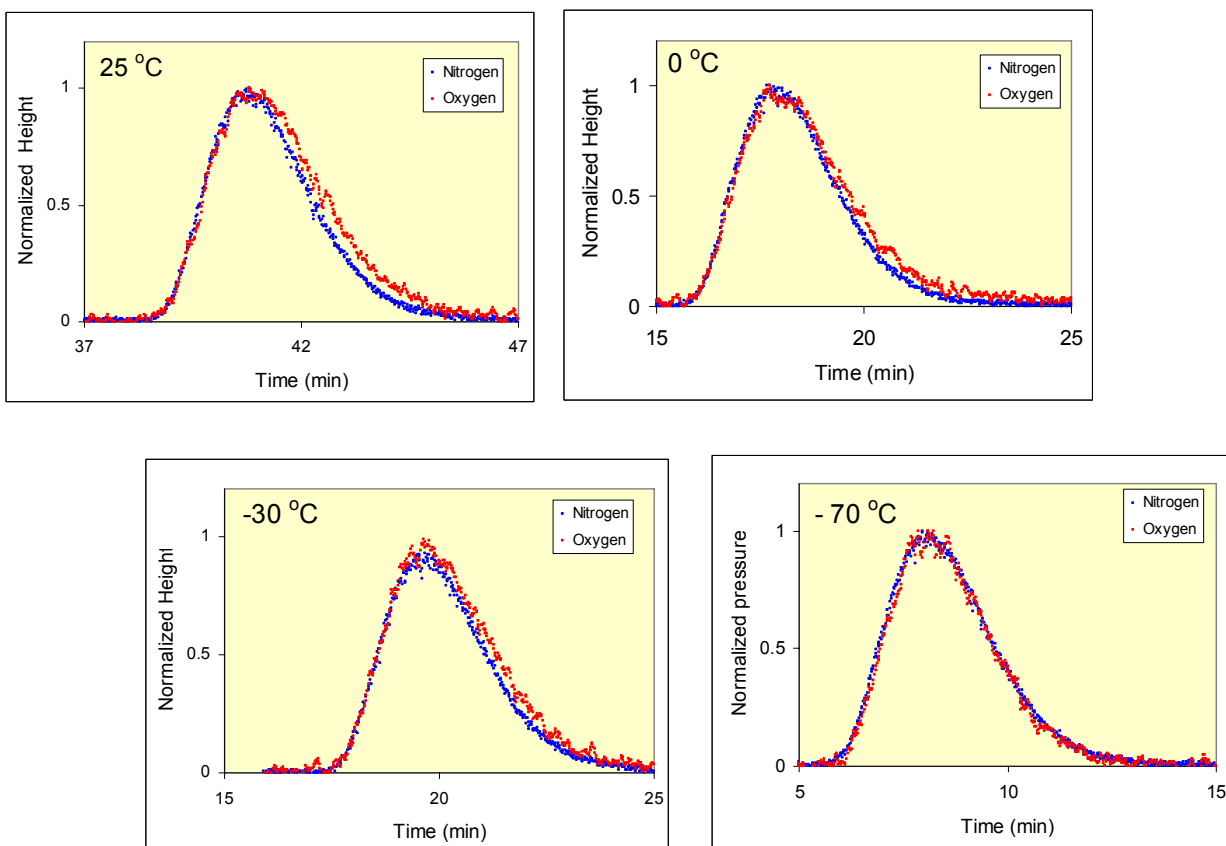


Figure 5: Normalized mass spectrometer signals for  $N_2$  (blue) and  $O_2$  (red) breaking through a 50 cm column packed with CFCMS K2-B material after injection of air at various temperatures. The flow rate of He was 15 cc/min.

A common trend observed by comparing the two sets of results is that lowering the temperature induces a gradual delay of the nitrogen peak with respect to the oxygen peak. The effect of temperature is greater for the TIM-2 material CFCMS sample for which the  $N_2$  peak is delayed more at lower temperatures. As shown in Fig. 2, TIM-2 has the largest volume of micropores in the 5 – 7 Å range (which is the range of pore widths efficient for molecular sieving separation of  $O_2$  and  $N_2$ ); larger micropores and small mesopores are also present. For this material there is little separation at room temperature, but separation is enhanced at lower temperatures. In contrast, although separation occurs even at room temperature on the CFCMS K2-B material, lowering the temperature causes the overlap of the two peaks. This material has a very narrow porosity distribution, with narrow micropores distributed in the 5 – 7 Å range (but with lower pore volume in this range); larger micropores and mesopores are absent. The results of Table 1 also show that the access of  $N_2$  to the internal porosity is more restricted on this material. The combination of

these factors determine the occurrence of  $N_2 - O_2$  separation at room temperature on the K2-B sample, which is thought to be caused by its narrow pore distribution. The reason why separation selectivity is gradually lost at low temperatures (Fig. 5) is probably blockage of narrowest pores by selective adsorption of gas molecules at low temperature.

## Zeolite

Zeolite 13X, with internal channel openings between 7.5 - 9 Å, is an industry standard for air separation and gas purification based on molecular sieving.<sup>[22,23]</sup> A sample of zeolite 13X (beads, 1.5-2 mm) was used in this project as a reference material. A temperature effect similar to that shown in Fig. 3 for CFCMS, though more clearly defined, was observed for this zeolite (Fig. 6). Although the column length used in this test was shorter (30 cm), air separation was more efficient, and improved greatly with lowering the temperature. However, common trend, also observed with CFCMS materials, was seen: lowering the temperature causes a delay of the nitrogen peak with respect to the oxygen one. This observation shows that the separation mechanism is the same for all three materials, i.e. it is based on kinetic separation during diffusion in narrow nanopores.

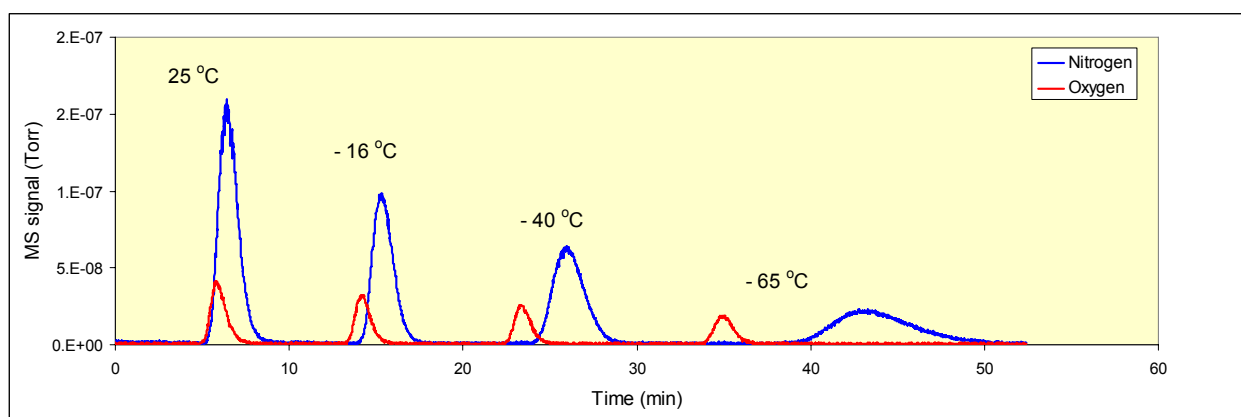


Figure 6: Mass spectrometer signals showing breakthrough of  $N_2$  (blue) and  $O_2$  (red) on zeolite 13X after injection of 5 mL air at various temperatures on. Flow rate of He carrier was 30 cc/min.

## INFLUENCE OF MAGNETIC FIELDS ON DYNAMIC AIR SEPARATION

All tests on effects of magnetic fields on dynamic air separation were carried out using gas chromatographic (GC) analysis; the instrument was equipped with a thermoconductivity detector and the carrier gas was He. Various materials, packed in chromatography-type columns as described above, were investigated in dynamic conditions; this included CFCMS samples TIM-2 and K2-B, magnetite-loaded CFCMS (Fe-NG-4), and zeolite X13 for reference. The flow conditions and the size of air injection were varied in an attempt to improve the separation. All tests were done at room temperature and atmospheric pressure.

When carbon materials (pure or loaded with  $Fe_3O_4$ ) were used, the delay of the  $N_2$  peak was not large enough as to afford separate detection of  $O_2$  and  $N_2$  peaks using the TC detector of the GC system. However, when a zeolite packed column was used, the nitrogen peak was delayed more compared with the oxygen one, and two distinct peaks were clearly identified by the TC detector (Fig. 7). For this system, several tests were done in an attempt to detect magnetic field effects. The zeolite column was placed between the poles of the water-cooled magnet, and identical air injections were done repeatedly with the magnetic field switched on and off. No differences were observed in the breakthrough times or the

magnitude of the two peaks (Fig. 7). Based on this result (and on many others, not reported here) the effect of magnetic fields on dynamic air separation on zeolite 13X was not confirmed.

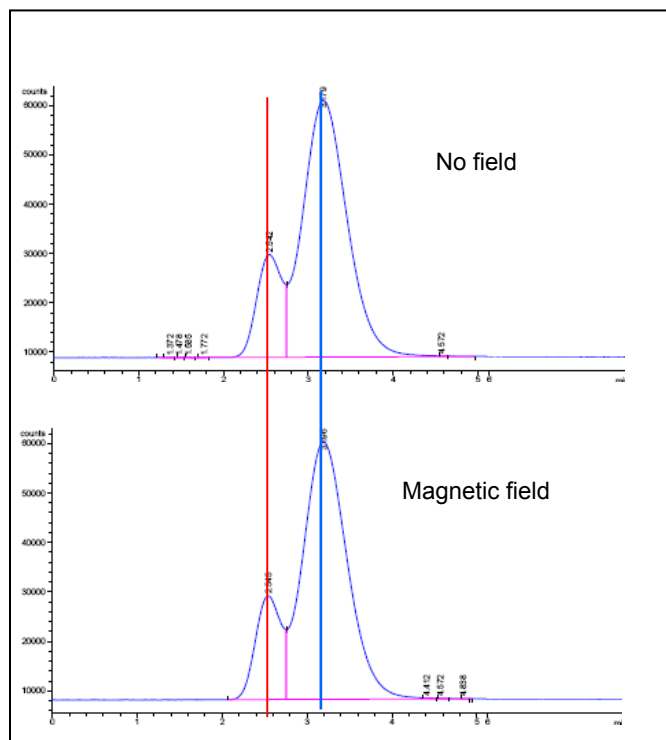


Figure 7: Example of air separation on zeolite 13X at room temperature (red – oxygen; blue – nitrogen). The flow rate of the carrier was 30 cc/min and the injection size was 0.1 cc. No detectable differences were seen between the cases with and without magnetic field (1.5 Tesla) applied.

## CONCLUSIONS

The findings reported here confirm that CFCMS materials have the potential for separating O<sub>2</sub> and N<sub>2</sub> from air on the basis of the different diffusion rates of the two molecules in the composite. The results show that in dynamic conditions, nitrogen diffusion through the extended pore system of microporous adsorbents is slower than that of oxygen, and become seven slower as the temperature is lowered. Carbon fiber molecular sieves have potential for N<sub>2</sub> - O<sub>2</sub> separation, provided better tailored porosity is developed, with pore widths comparable to molecular dimensions. This depends on identifying and demonstrating alternative techniques of activation, and using new carbon precursors (such as lignine) that are known to produce extensive networks of uniformly narrow micropores. The effect of magnetic fields on air separation was not confirmed at room temperature for zeolite 13X and for Fe<sub>3</sub>O<sub>4</sub>-loaded CFCMS in dynamic conditions. At this moment it is unclear whether this conclusion can be generalized, given the fact that this finding in dynamic conditions contradicts previous results obtained in static (equilibrium) conditions. These data require more sophisticated measurements, using much higher intensity magnetic fields, to verify the preliminary results and determine whether magnetic fields can be exploited for separation of O<sub>2</sub> and N<sub>2</sub> from air. Furthermore, as current results show, efficient air separation is achievable on zeolite. There is a large potential for further development by combining air separation on zeolite with second-stage purification or oxygen enrichment on carbon molecular sieves, notably CFCMS, to exploit the electrical swing adsorption capability of these materials.

## ACKNOWLEDGEMENTS

Research sponsored by Office of Fossil Energy, U.S. Department of Energy, National Energy Technology Laboratory, under the Fossil Energy Advanced Research Materials Program, contract number DE-AC05-00OR22725 with UT-Battelle, LLC.

## REFERENCES

1. Burchell, T. D., Judkins, R. R., Rogers, M. R., and Williams, A. M., A Novel Process for the Separation of Carbon Dioxide and Hydrogen Sulfide for Gas Mixtures, *CARBON*, **35** (1997) 1279-1294.
2. Burchell, T. D., Weaver, C. E., Chilcoat, B. R., Derbyshire, F., and Jagtoyen, M., Activated Carbon Fiber Composite Material and Method of Making, U.S. Patent 6,030,698 (February 29, 2000) Assigned to Lockheed Martin Energy Research Corporation.
3. Burchell, T. D., Weaver, C. E., Chilcoat, B. R., Derbyshire, F., and Jagtoyen, M., Activated Carbon Fiber Composite Material and Method of Making, U.S. Patent 6,258,300 (July 10, 2001) Assigned to UT-Battelle, LLC.
4. Burchell, T. D., and Judkins, R. R., A Novel Carbon Fiber Based Material and Separation Technology, *Energy Conservation and Management*, **38** Supplement, S99-S10 (1997).
5. Wilson, K. A., Burchell, T. D., and Judkins, R. R., Carbon Fiber Composite Molecular Sieve Electrically Regenerable Air Filter Media, U. S. Patent 5,827,355, (October 27, 1998), Assigned to Lockheed Martin Energy Research Corporation.
6. Judkins, R. R., and Burchell, T. D., Gas Separation Device Based on Electrical Swing Adsorption, U. S. Patent 5,972,077 (October 26, 1999) Assigned to Lockheed Martin Energy Research Corporation.
7. Burchell, T. D., Omatete, O., Gallego, N. C., and Baker, F. S., Novel Activated Carbon Composites for Air Separation, *Proceedings of the 18th Annual Conference on Fossil Energy Materials*, Knoxville, TN, June 2-4, 2004.
8. Kaneko, K., Fukuzaki, N., and Ozeki, S., The Concentrated NO Dimer in Micropores Above Room Temperature, *J. Chem. Phys.*, **87** (1987) 776-777.
9. Takaishi, Y., Dimers of Oxygen Molecules in the Pores of Ca<sub>6</sub>A Zeolite, *J. Chem. Soc. Faraday Trans.*, **93** (1997) 1257-1260.
10. Yamamoto, I., Yamaguchi, M., Goto, T., and Miura, S., Chemical Equilibrium of the Ferromagnetic LaCo-H<sub>5</sub> System in Strong Magnetic Fields, *J. Alloys Compounds*, **231** (1995) 205-207.
11. Ozeki, S., Wakai, C., and Ono, S., Is Magnetic Effect on Water Possible?, *J. Phys. Chem.*, **95** (1991) 10557-10559
12. Miyamoto, J., Matsubara, Y., Kurashima, H., Tazaki, T., and Ozeki, S., Magnetic Field Effects on Physical Adsorption Equilibrium Between Solids and Gases of Organic Molecules and Oxygen, *Nippon Kinzoku Gakkaishi*, **61** (1997) 1300-1305.
13. Ozeki, S., and Sato, H., Magnetic Interactions in Adsorption at Solid Surfaces, in *Encyclopedia of Surface and Colloid Science*, Marcel Dekker, New York, pp. 3120-3131 (2002).
14. Baker, F. S., Contescu, C. I., Tsouris, C., and Burchell, T. D., Activated Carbon Composites for Air Separation, *Proceedings of the 20th Annual Conference on Fossil Energy Materials*, Knoxville, TN, June 12-14, 2006.
15. Brunauer, S., Emmett, P. H., and Teller, E., Adsorption of Gases in Multimolecular Layers, *J. Am. Chem. Soc.*, **60** (1938) 309-319.
16. Gregg, S. J., and Sing, K. S. W., "Adsorption, Surface Area and Porosity", 2<sup>nd</sup> Edition, Academic Press, London (1982).
17. Lastoskie, C., Gubbins, K. E., and Quirke, N., Pore Size Distribution Analysis of Microporous Carbons: A Density Functional Theory Approach, *J. Phys. Chem.*, **97** (1993) 4786-479.

18. Jagiello, J., and Thommes, M., Comparison of DFT Characterization Methods Based on N<sub>2</sub>, Ar, CO<sub>2</sub>, and H<sub>2</sub> Adsorption Applied to Carbons with Various Pore Size Distributions, *CARBON*, **42** (2004) 1227-1232.
19. Rodriguez-Reinoso, F. and Linares-Solano, A., Microporous Structure of Activated Carbons as Revealed by Adsorption Methods, in “*Chemistry and Physics of Carbon*”, Edited by P. A. Thrower, Volume 21, pp. 1-146, Marcel Dekker, New York (1988).
20. Baker, F. S., Contescu, C. I., Tsouris, C., Gallego, N. C., and Burchell, T. D., Carbon Fiber Composite Molecular Sieve for Air Separation, *Extended Abstracts, Carbon 2006 International Conference*, Aberdeen, Scotland, July 16-21, 2006.
21. Spacu, P., Brezeanu, M., Patron. L., Contescu, A., and Crisan, D., Coordination Compounds as Raw Materials for Mixed Oxides, *Thermochimica Acta*, **178** (1991) 231-239.
22. Jee, J.-G., Lee, J.-S., and Lee, C.-H., Air Separation by a Small Scale Two-Bed Medical O<sub>2</sub> Pressure Swing Adsorption, *Ind. Eng. Chem. Res.* **40** (2001) 3647-3658.
23. Jee, J.-G., Lee, S.-J., Moon, H.-M., and Lee, C.-H., Adsorption Dynamics of Air on Zeolite 13X and CMS Beds for Separation and Purification, *Adsorption* **11** (2005) 415-420.